IEEE Access
Multidisciplinary | Rapid Review | Open Access Journal

Received February 10, 2020, accepted March 3, 2020, date of publication March 6, 2020, date of current version March 17, 2020.

Digital Object Identifier 10.1109/ACCESS.2020.2978883

Evasive Maneuver Strategy for UCAV in Beyond-Visual-Range Air Combat Based on Hierarchical Multi-Objective Evolutionary Algorithm

ZHEN YANG, DEYUN ZHOU, HAIYIN PIAO, KAI ZHANG, WEIREN KONG, AND QIAN PAN

School of Electronics and Information, Northwestern Polytechnical University, Xi'an 710072, China

Corresponding author: Zhen Yang (nwpuyz@foxmail.com)

This work was supported in part by the National Natural Science Foundation of China under Grant 61603299 and Grant 61612385, and in part by the Fundamental Research Funds for the Central Universities under Grant 3102019ZX016.

ABSTRACT This study deals with the autonomous evasive maneuver strategy of unmanned combat air vehicle (UCAV), which is threatened by a high-performance beyond-visual-range (BVR) air-to-air missile (AAM). Considering tactical demands of achieving self-conflicting evasive objectives in actual air combat, including higher miss distance, less energy consumption and longer guidance support time, the evasive maneuver problem in BVR air combat is defined and reformulated into a multi-objective optimization problem. Effective maneuvers of UCAV used in different evasion phases are modeled in three-dimensional space. Then the three-level decision space structure is established according to qualitative evasive tactical planning. A hierarchical multi-objective evolutionary algorithm (HMOEA) is designed to find the approximate Pareto-optimal solutions of the problem. The approach combines qualitative tactical experience and quantitative maneuver decision optimization method effectively. Simulations are used to demonstrate the feasibility and effectiveness of the approach. The results show that the obtained set of decision variables constitutes nondominated solutions, which can meet different evasive tactical requirements of UCAV while ensuring successful evasion.

INDEX TERMS BVR air combat, evasive maneuver, hierarchical evolutionary algorithm, multi-objective optimization, UCAV.

I. INTRODUCTION

With the rapid development of artificial intelligence technology and its in-depth application in the military field, the combat mission of unmanned combat air vehicle (UCAV) has gradually expanded from the current airborne intelligence, surveillance & reconnaissance [1], close air support, and electronic support measure to the field of air combat. Beyond-visual-range (BVR) air combat is the main form of fighting for air superiority at present. The mode that UCAV serves as an aerial "shooter" in BVR air combat can avoid complicated dogfight. Advanced tactical data link, airborne avionics, and BVR air-to-air missile (AAM) laid the foundation for this air combat mode [2].

The associate editor coordinating the review of this manuscript and approving it for publication was Baoping Cai.

Compared with high-dynamic and intense confrontation of the dogfight, the rhythm of BVR air combat is relatively moderate, where more emphasis is placed on tactical planning. Security is the basis and prerequisite of realizing all missions, and high-efficiency evasive maneuver strategy is the key to improve survival probability for UCAV, which is threatened by a high-performance BVR AAM. Compared with the manned fighter, UCAV does not need to consider the physical and mental constraints of pilots. Its flight performance and control accuracy are more superior, it can process and analyze various situation data more quickly and efficiently. All of these provide more advantages for UCAV in evasion.

Since the AAM was first deployed in actual combat, the evasive maneuver strategy of a fighter against AAM has been one of the key research issues in the field of air combat.

Many approaches, such as differential games [3]–[6], optimum control [7]–[11], model predictive control [12]–[15], and evolutionary algorithms [16]–[21], have been applied to obtain the optimal or approximate optimal evasive maneuver command for a fighter.

Imado and Miwa [22], [23] made a comparative study of several evasive maneuvers against the proportional navigation missile. It was shown that each maneuver had its advantageous region and the evasion strategy should change depending on relative geometry relationship. Some features of the high-g barrel (HGB) roll and split-S maneuvers, and the effects of the parameters on the miss distance (MD) were studied through mathematical simulation [24], [25]. On this basis, Akdag and Altilar [26], [27] analyzed the evasive effects between the maneuver combinations of Immelmann followed by a HGB and split-S followed by a HGB.

To obtain the analytic solution of optimal maneuver, the problem could be formulated as a two-sided optimization called a zero-sum two-person differential game [3], [6]. It was solved by semidirect collocation with nonlinear programming in [3]. Carr *et al.* [4] obtained an initial guess for the physically unintuitive costates through solving a one-sided optimal control problem. This study was extended in [5] to a family of local solutions, and Alkaher and Moshaiov [6] also solved this game through an optimal controller in a closed-loop form, which resulted in a safe-navigation strategy for the fighter.

Optimal control theory is also an effective solution in the evasion problem [7]–[11]. Imado [7], [8] proposed some practical approaches to the construction of suboptimal strategies of the behavior of players for different data on the choice of controls by their opponents. This study was extended in [9] to evade two missiles simultaneously, which based on the steepest ascent method. Ong and Pierson [10], [11] treated the evasion problem as an approximated parameter optimization problem, and sequential quadratic programming was used to solve it.

The closed-loop method based on optimal control is affected by the disaster phenomenon of dimensionality. In general, it is only suitable for highly simplified problems, and this motivates other studied approaches. Karelahti *et al.* [12] presented a receding horizon control scheme for obtaining near-optimal controls in a feedback form. Furthermore, online identification method of the guidance law of the missile for the control scheme was addressed in [13]. A similar problem was solved in [14], [15] by nonlinear model predictive control, which was another strategy for computing near-optimal feedback control based on current state information.

Some scholars have tried to use the intelligent optimization algorithm to solve the global optimal solution of the problem, because it opens up the possibility to search for an optimal solution with the presence of nonlinearity, parameter discontinuity, and discrete input [16]. Moore and Garcia [17], [18] described the implementation of a genetic programming system that evolved optimized solutions to the pursuer/evader problems. Nusyirwan and Bil [16], [19] proposed a technique using a parallel evolutionary algorithm to search for optimal control for an evasive fighter. A similar scheme was applied in [20] and [21], which used a co-evolutionary augmented lagrangian method and quantum-behaved particle swarm optimization algorithm, respectively. There were also some artificial intelligence methods such as neural networks [28] and reinforcement learning [29] applied to solve the problem. In addition, a more innovative approach involves decoy deployment [30] and protecting fighter by using a defender missile (see [31], [32]).

The aforementioned literature mostly deals with a situation, in which the fighter is already located within the missile's guaranteed kinetic-capture zone (GKZ), which was called ''endgame evasion'' in [33]. The above approaches have achieved satisfactory evasion effects in this situation, but they are not fully applicable to evade BVR AAM, which often lanches as the opponent is far from the GKZ. The latter studies focus more on recommending to the fighter how to apply tactical planning rather than dynamic advantages.

The experience and knowledge summarized from numerous air combat cases and widely accepted among pilots are very effective for this problem, but they were rarely reflected in traditional methods. What's more important is that BVR evasion usually has multiple tactical objectives in actual air combat, not just MD. For example, prolonging the guidance support time (GST) means increasing the probability of hitting the target. Maximizing the MD means increasing the survival probability [34]. Besides, decreasing energy consumption (EC) means UCAV has more energy for subsequent combat after a successful evasion. So this problem that involves three self-conflicting objectives has no unique optimal solution but rather a set of Pareto-optimal strategies [35], and strategy choice should be decided by UCAV's mission commands or current battlefield situation.

To solve the aforementioned problem, a hierarchical multi-objective evolutionary algorithm (HMOEA) is designed in this paper, which combines qualitative tactical experience and quantitative maneuver decision optimization method. Firstly, three-dimensional maneuver models are presented for different intentions in different BVR evasion phases. Then the three-level decision space structure is established according to qualitative evasive tactical planning, which includes timing, type, and parameters of evasive maneuvers. Next, the optimization model of the evasive maneuver strategy for UCAV in BVR air combat is established based on the three objective function models and corresponding constraints. Finally, a redesigned multi-objective evolutionary algorithm based on decomposition (MOEA/D) [36] is proposed to solve the model through the design of normalized decomposition and hierarchical evolutionary mechanism. The simulation results demonstrate the strength and practicability of the proposed method. It also effectively overcome defects that the decision-making period is difficult to determine and the result is difficult to explain in traditional methods. To the best of our knowledge, this is the first time the problem of evasive strategy in BVR air combat is addressed in the open

literature using the HMOEA and corresponding mathematics models.

The rest of this paper is organized as follows. In Section II, the evasive maneuver problem in BVR air combat is defined and reformulated into the multi-objective optimization problem. The details of the HMOEA are presented in Section III. The proposed models and algorithm are demonstrated with simulation experiments in Section IV, followed by conclusion and future work in Section V.

II. PROBLEM FORMULATION

Dogfight emphasizes the game of space angle. However, BVR air combat usually starts from a head-on geometry with a large distance. The condition of space angle for launching missile is easier to meet, and there is more of an emphasis on the distance game. As we all know, principles of first detection, first shot, first hit and first leave are the key to improve both the air superiority and survival probability in BVR air combat. Therefore, the problem of evasive strategy in BVR air combat not only need to keep the aircrafte from being hit, but also need to consider the whole battle efficiency and tactical superiority.

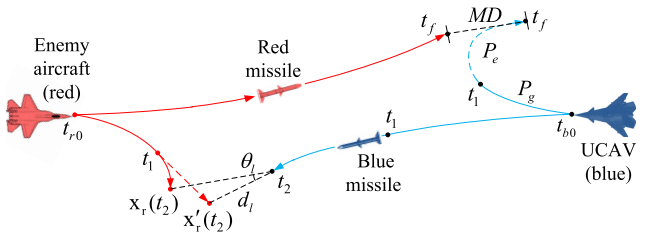

FIGURE 1. Scenario of one-on-one BVR air combat.

A. PROBLEM ANALYSIS

This paper considers a common scenario of one-on-one BVR air combat as shown in Fig. 1. The UCAV launches the blue BVR AAM (abbreviated as BM) toward the red enemy aircraft (abbreviated as RA) at t_{b0}. Note that RA also launches the red BVR AAM (abbreviated as RM) at t_{r0}. It is assumed that both sides launch missile at approximately the same time, namely $t_{b0} \approx t_{r0}$. UCAV starts the phase of guidance support P_g immediately after the launch. The BM obtains RA's information through an uplink from the UCAV which tracks the RA. At t_1, UCAV finishes supporting BM and starts the evasive phase P_e to evade RM. Then, the BM stops receiving RA's information. Therefore, BM extrapolates the RA's trajectory with the latest available RA's information by assuming that the RA flies at constant velocity and direction. At t_2, the BM reaches the maximal lock-on distance d_l to the extrapolated position of the RA, whereupon it switches on its own radar with an attempt to lock on the RA. At that moment, there is an angle of tracking error θ_l between the true and estimated line-of-sight from BM to the real $x_r(t_2)$ and estimated position $x'_r(t_2)$ of RA (see Fig. 1). θ_l is an important factor that affects the intercept and hit probability of BVR AAM [34]. During the phase P_e, UCAV tries to maximize the MD at the terminal time t_f by using a series of evasive maneuvers. MD is the key to ensuring the survival probability of UCAV.

As can be seen from the above process, prolonging the phase P_g (i.e., GST) and reducing extrapolation time of the BM can effectively decrease θ_l, which thereby increase the hit probability of the BM. Ideally, BM's range to $x_r(t_2)$ is less than d_l at t_1. Then BM does not need to estimate the RA's information, so the hit probability is relatively high. But it also means reducing the time spent in the phase P_e, which will results in significantly increasing the threat of RM and reducing the survival probability of UCAV. Conversely, if UCAV starts the phase P_e early, which will results in higher survival probability and lower hit probability. Therefore, the choice of t_1 reflects the different tactical tendencies of UCAV. Besides, during the phase P_e, when and what evasive maneuver is adopted, as well as the size of maneuver parameters are also the core of evasive strategy. It will affect the MD and also lead to different levels of EC. Less EC means more energy is available for subsequent air combat after a successful evasion, thereby creating more tactical superiority for UCAV.

Accoring to the aforementioned analysis, the evasive maneuver problem in BVR air combat is defined and reformulated into a multi-objective optimization problem in this paper, which includes multi-dimensional decision variables. The flowchart of the solution approach is shown in Fig. 2. It includes the evasion model (as illustrated in the left-side panel of Fig. 2) and the optimization model (as illustrated in the right-side panel of Fig. 2). The evasion model implements the following steps: establishing dynamics and constraints of UCAV and missile, according to the qualitative evasive tactical planning to design the initial decision space. The optimization model implements the following steps: hierarchical initialization of the decision space, generating quantitative evasive tactical planning, solving the objective space (i.e., MD, EC, and GST) by digital simulation of evasive behavior, then a multi-objective hierarchical evolutionary algorithm is designed to find the approximate Pareto-optimal strategy set of evasive maneuver.

Before modeling, for the scenario in Fig. 1, several assumptions that simplify the problem to a certain extent without losing practicability are listed:

1. Both sides can obtain real-time status information of each other and missiles they launch.
2. Both sides launch the missile when the opponent is far from the respective GKZ.
3. During the phase of guidance support, the UCAV close to the RA using initial velocity and direction.
4. There is no consideration given to the case of adopting active or passive jamming measures.

B. "Missile-UCAV" MODELING

1) RELATIVE MOTION MODEL

Firstly, the relative motion relationship between the missile and UCAV is established in three-dimensional space, as shown in Fig. 3.

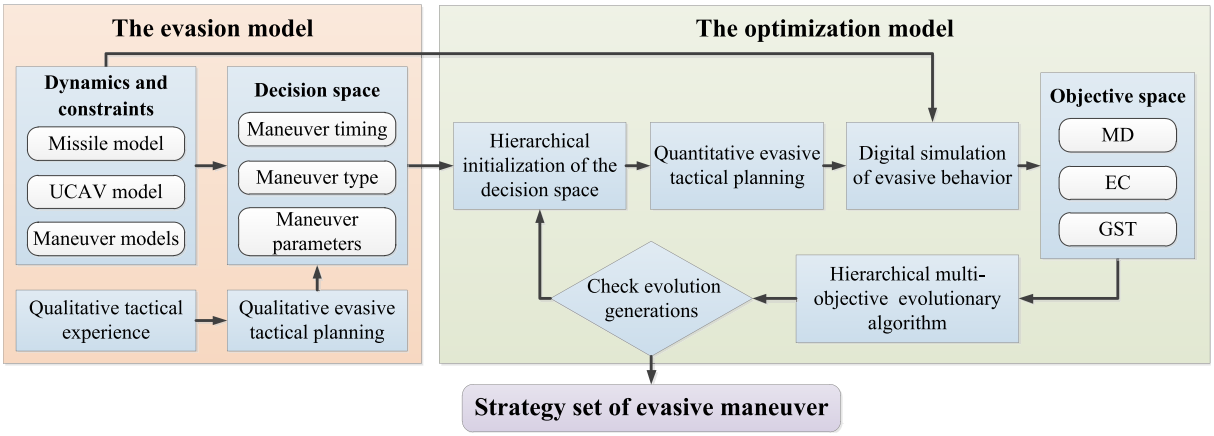

FIGURE 2. The flowchart of the solution approach.

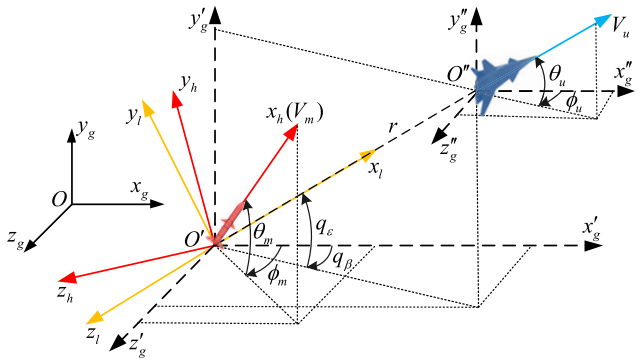

FIGURE 3. Relative motion relationship between the missile and UCAV.

In Fig. 3, $Ox_gy_gz_g$, $O'x'_gy'_gz'_g$, $O''x''_gy''_gz''_g$, $O'x_hy_hz_h$, and $O'x_ly_lz_l$ refer to the geographic coordinate system, the concomitant inertial coordinate system of the missile, the concomitant inertial coordinate system of the UCAV, the trajectory coordinate system of the missile and the line-of-sight coordinate system of the missile, respectively. θ_m, ϕ_m, θ_u and ϕ_u are the flight path angle and the heading angle of the missile and UCAV, respectively. q_ε and q_β are the inclination angle and the deflection angle of line-of-sight of the missile, respectively. The remaining state variables are the distance r between the missile and UCAV, the missile's velocity V_m, and UCAV's velocity V_u. Besides, the subscript m and u represent the missile and the UCAV, respectively (similarly hereinafter).

For unified modeling analysis and calculating the missile's guidance command, the relative motion model of the missile and UCAV is established by the following system of differential equations:

$$\dot{r} = \frac{x_r\dot{x}_r + y_r\dot{y}_r + z_r\dot{z}_r}{r} \tag{1}$$

$$\dot{q}_\varepsilon = \frac{(x_r^2 + z_r^2)\dot{y}_r - y_r(\dot{x}_r x_r + \dot{z}_r z_r)}{r^2\sqrt{x_r^2 + z_r^2}} \tag{2}$$

$$\dot{q}_\beta = \frac{\dot{z}_r x_r - \dot{x}_r z_r}{x_r^2 + z_r^2} \tag{3}$$

where

$$r = \sqrt{x_r^2 + y_r^2 + z_r^2} \tag{4}$$

Besides, $x_r = x_u - x_m$, $y_r = y_u - y_m$, $z_r = z_u - z_m$, $\dot{x}_r = \dot{x}_u - \dot{x}_m$, $\dot{y}_r = \dot{y}_u - \dot{y}_m$, and $\dot{z}_r = \dot{z}_u - \dot{z}_m$. x_u and z_u refer to the horizontal coordinates and y_u to the altitude of the UCAV. Similarly, x_m, y_m, and z_m refer to the corresponding position coordinates of the missile.

2) MISSILE MODEL

The dynamics of the missile used in this study is described by a simplified sixth-order point-mass model, the equations of motion are

$$\begin{cases} \dot{x}_m = V_m \cos\theta_m \cos\phi_m \\ \dot{y}_m = V_m \sin\theta_m \\ \dot{z}_m = V_m \cos\theta_m \sin\phi_m \\ \dot{V}_m = (P_m(t) - D_m)/m_m(t) - g\sin\theta_m \\ \dot{\theta}_m = (n_{my} - cos\theta_m)g/V_m \\ \dot{\varphi}_m = n_{mz}g/(V_m\cos\theta_m) \end{cases} \tag{5}$$

The mass of the missile $m_m(t)$ and the thrust force $P_m(t)$ are functions of the missile's flight time t. The maximum engine operating time is set as t_p. g is the acceleration of gravity. The drag force D_m is given as tabular data, which is determined by the missile's current altitude, velocity, and reference wing area, etc. n_{my} and n_{mz} are the overload control commands of the missile in pitch and yaw channels, respectively. According to the proportional navigation guidance scheme, the guidance law can be stated as

$$\begin{cases} n_{myc} = (N_m|\dot{r}|\dot{q}_\varepsilon)/g + 1.0 \\ n_{mzc} = (N_m|\dot{r}|\dot{q}_\beta)/g \end{cases} \tag{6}$$

where N_m is the navigation constant. n_{myc} and n_{mzc} are the required overload of the missile in the pitch and yaw channels, respectively. Considering the overload constraint, they are given as follows:

$$\begin{cases} |n'_{myc}| = \min(n_{\max}, n_m)n_{myc}/n_m \\ |n'_{mzc}| = \min(n_{\max}, n_m)n_{mzc}/n_m \end{cases} \tag{7}$$

where

$$n_m = \sqrt{{n_{myc}}^2 + {n_{mzc}}^2} \tag{8}$$

and $n_{\max}$ is the maximum available overload of the missile in the normal direction. n'_{myc} and n'_{mzc} are required overloads with the constraint. Finally, the overload control commands are given through first-order lag from command signals:

$$\begin{cases} \dot{n}_{my} = (n'_{myc} - n_{my})/\tau_m \\ \dot{n}_{mz} = (n'_{mzc} - n_{mz})/\tau_m \end{cases} \tag{9}$$

where τ_m is the missile time constant.

3) UCAV MODEL

This study focuses on the influence of UCAV's trajectory on evasive effects. In order to avoid introducing much complicated aerodynamic parameters in the algorithm, as well as for preferable computing efficiency and universality of strategy set, a simplified model represented by constrained overload is used to solve the evasive trajectory of UCAV in this paper. The motion of the UCAV is described by

$$\begin{cases} \dot{x}_u = V_u \cos\theta_u \cos\phi_u \\ \dot{y}_u = V_u \sin\theta_u \\ \dot{z}_u = V_u \cos\theta_u \sin\phi_u \\ \dot{V}_u = (n_x - \sin\theta_u)g \\ \dot{\theta}_u = (n_y - cos\theta_u)g/V_u \\ \dot{\varphi}_u = n_z g/(V_u \cos\theta_u) \end{cases} \tag{10}$$

where n_x, n_y and n_z are control vectors of the UCAV, which are the overload component of the corresponding axis of the UCAV in the trajectory coordinate system. The overload rate are $|\dot{n}_x| = a_1$ and $|\dot{n}_y| = |\dot{n}_z| = a_2$, where a_1 and a_2 are constant.

Equation (10) is constrainted by

$$\begin{cases} |n_x| \le n_{x\max} \\ \sqrt{{n_y}^2 + {n_z}^2} \le n_{n\max} \\ y_{u\min} \le y_u \le y_{u\max} \\ V_{u\min} \le V_u \le V_{u\max} \end{cases} \tag{11}$$

where $n_{x\max}$ and $n_{n\max}$ are the maximum available overload of the UCAV in the tangential and normal direction, respectively. $y_{u\min}$ and $y_{u\max}$ are safe flight altitude boundary of the UCAV, $V_{u\min}$ and $V_{u\max}$ are safe flight velocity boundary of the UCAV.

4) EVASIVE MANEUVER MODELS

Evasive maneuver models of the UCAV are established according to the characteristics of BVR air combat in this section. Refer to effective qualitative tactics summarized from a large number of air combat cases, evasive maneuvers commonly used in BVR air combat boil down to four types in this paper, include turning, altitude, period, and terminal.

a: TURNING TYPE

Turning type maneuvers are generally used in the initial evasive phase with a head-on situation, of which tactical purpose is minimizing the closing velocity with the incoming missile and changing the interception geometry from a head-on to a tail-chase geometry. These maneuvers include out, abort, and split-S maneuver, and corresponding maneuver trajectories are demonstrated in Fig. 4. The coordinate labels in Fig. 4 refer to the corresponding coordinate axes in the geographic coordinate system in Fig. 3 (similarly hereinafter). Turning efficiencies of these three maneuvers are increasing successively, but the EC of the UCAV also increases accordingly.

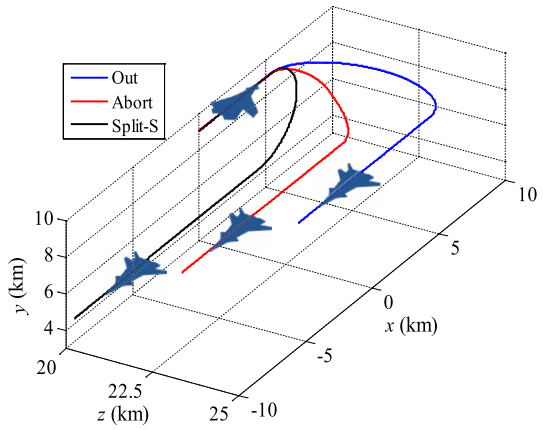

FIGURE 4. Maneuver trajectories of turning type.

To reduce the closing velocity with the incoming missile and improve the turning efficiency, UCAV usually turns with deceleration which is controlled by

$$n_{xc} = \begin{cases} -n_{xd}, & V_u > V_{ud} \\ \sin\theta_u, & V_u \le V_{ud} \end{cases} \tag{12}$$

where V_{ud}, n_{xc}, and n_{xd} are velocity command, actual overload control variable in the tangential direction, and overload command in the tangential direction, respectively. Note that $n_{xd} \in [0, n_{x\max}]$ and n_{xc} switches with a rate of change as $n_{xc} = n_x \pm a_1 \cdot \Delta t$. Similarly, actual control variable of overload in the pitch and yaw channels, which are denoted as n_{yc} and n_{zc}, respectively, switch with the overload rate a_2 (similarly hereinafter).

The out maneuver refers to the horizontal turn with a constant or varying radius of curvature, which turning efficiency is relatively low but EC is preferable. Its control method in the yaw channel is given as

$$n_{zc} = \begin{cases} n_{zd}, & |\phi_u - \phi_{u0}| < \phi_{ud} \\ 0, & |\phi_u - \phi_{u0}| \ge \phi_{ud} \end{cases} \tag{13}$$

where n_{zd}, ϕ_{u0}, and ϕ_{ud} are overload command in the yaw channel, initial heading angle, and turning angle command, respectively. Besides, the UCAV keeps $n_{yc} = 1$ and $\theta_u = 0$ during the turn.

The abort maneuver keeps turning back to the tail with an overload in the normal direction, which aims to reduce the turning radius and improve turning efficiency. So it will reduce the altitude and velocity of the UCAV. The control method of the maneuver in the yaw channel is the same as (13). To realize horizontal flight after finishing the command ϕ_{ud}, the control method of the abort maneuver in the pitch channel is designed as

$$n_{yc} = \begin{cases} -n_{yd} + cos\theta_u, & |\phi_u - \phi_{u0}| < \phi_{ud}/2 \\ n_{yd} + cos\theta_u, & |\phi_u - \phi_{u0}| \geq \phi_{ud}/2 \wedge \theta_u < 0 \\ 1, & |\phi_u - \phi_{u0}| \geq \phi_{ud}/2 \wedge \theta_u \geq 0 \end{cases} \tag{14}$$

where n_{yd} is overload command in the pitch channel, and $cos\theta_u$ is a gravity compensation term. To reduce the complexity of the following optimization algorithm, the command is given as $n_{yd} = n_{zd}$.

The split-S maneuver consists of a half-roll followed by a tight vertical loop downwards, which begins with rolling 180 *deg*, once upside down, pulling back on the stick to execute a vertical U-turn [26]. That can minimize closing velocity with the incoming missile to the maximum extent possible and quickly achieve the tail-chase intention. The control method of the split-S maneuver in the pitch channel is designed as

$$n_{yc} = \begin{cases} -n_{yd} + cos\theta_u, & \theta_u > -\pi \\ 1, & \theta_u \leq -\pi \end{cases} \tag{15}$$

Besides, the UCAV keeps n_{zc}= 0 during the maneuver.

b: ALTITUDE TYPE

Altitude type maneuvers refer to descend the flight altitude by diving under a safe altitude condition, of which tactical purpose is to make the incoming missile to dive to the ground and increasing D_m through greater air density in lower altitudes. Thereby consuming the missile's energy more effectively. Moreover, the missile's seeker would also be disturbed by ground clutter to some extent in this way [34]. However, this also means the reduction of energy and tactical superiority in BVR air combat. Altitude type maneuvers include altitude hold, straight dive (abbreviated as L-Dive), and S-shaped dive (abbreviated as S-Dive) in this paper, corresponding maneuver trajectories are demonstrated in Fig. 5.

The motion with constant or increased velocity is generally used in altitude type maneuvers, which velocity control method is similar to (12)

$$n_{xc} = \begin{cases} n_{xd}, & V_u < V_{ud} \\ \sin\theta_u, & V_u \geq V_{ud} \end{cases} \tag{16}$$

It's worth noting that if the incoming missile is relatively far away, the UCAV can evade the missile through a horizontal flight with a constant or increased velocity, i.e., altitude hold. In this case, UCAV just needs to keep $n_{yc} = 1$ and $n_{zc} = 0$.

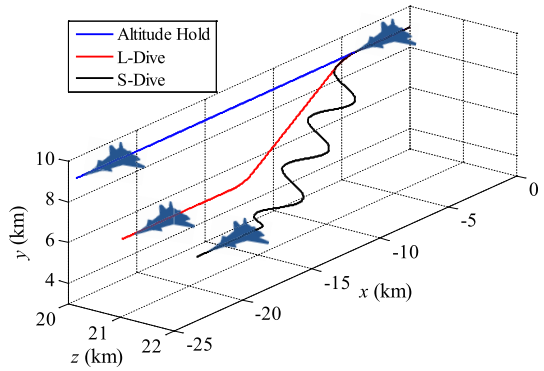

FIGURE 5. Maneuver trajectories of altitude type.

The L-Dive maneuver refers to dive with a constant flight path angle. Firstly, The UCAV starts the dive from horizontal flight by control the n_{yc}. When the preset flight path angle θ_{ud} is reached, the UCAV starts the straight dive phase, then pull-out in advance before reaching the desired altitude H_d. Finally, the L-Dive maneuver ends up with a horizontal flight. The control method of the maneuver in the pitch channel is designed as

$$n_{yc} = \begin{cases} -n_{yd} + \cos\theta_u, & H > H_d + \Delta H \wedge |\theta_u - \theta_{u0}| < \theta_{ud} \\ \cos\theta_u, & H > H_d + \Delta H \wedge |\theta_u - \theta_{u0}| \geq \theta_{ud} \\ n_{yd} + \cos\theta_u, & H \leq H_d + \Delta H \wedge \theta_u < 0 \\ 1, & H \leq H_d + \Delta H \wedge \theta_u \geq 0 \end{cases} \tag{17}$$

where θ_{u0} is the initial flight path angle. $\Delta H = (1 - \cos\theta_d) \cdot R_d$ is the altitude loss during pull-out, where R_d is the radius of curvature of pull-out. R_d is simplified to a constant in this paper, i.e., $R_d = {V_u}^2/g{\cdot}n_{yd}$. Besides, the UCAV keeps n_{zc}= 0 during the maneuver.

The S-Dive maneuver is the combination of dive and horizontal S-shaped maneuvers, that is, changing the above straight dive mode to S-shaped dive. In the control method, let $n_{zc} = n_{zd} \cdot \cos(\omega_{d1} \cdot t)$, where ω_{d1} is the angular velocity in the S-Dive maneuver. n_{zc} is still equal to zero in the other phase.

c: PERIOD TYPE

Period type maneuvers refer to generating the horizontal S-shaped (abbreviated as S-Plane) or barrel roll trajectory through changing the overload direction periodically, corresponding maneuver trajectories are demonstrated in Fig. 6. Such maneuvers force the incoming missile to constantly maneuver in different directions. Because of the missile's pursuit mode, it is necessary to re-establish the lead pursuit every time when the target changes course, which greatly increases the missile's flight distance and consumes its kinetic energy. Moreover, that will accumulate the missile's delay error continuously, thus generating a larger dynamic error and increasing the MD.

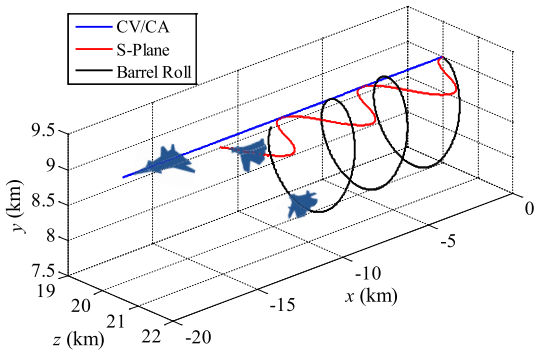

FIGURE 6. Maneuver trajectories of period type.

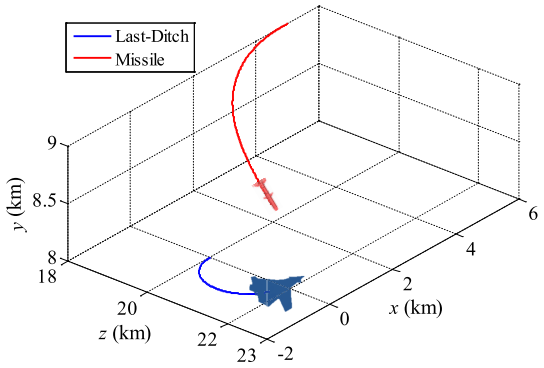

FIGURE 7. Maneuver trajectories of terminal type.

Similar to the situation of altitude hold, if there is enough distance to evade the incoming missile, the constant overload maneuvers could be chosen to decrease EC, i.e., flying with constant velocity (CV) or constant acceleration (CA). The velocity control method is similar to (16). Besides, let $n_{yc}= 1$ and $n_{zc}= 0$.

The S-Plane maneuver is a periodic turning maneuver with the S-shaped trajectory in a horizontal plane. The control method of the maneuver in the yaw channel is given as $n_{zc} = n_{zd} \cdot \cos(\omega_{d2} \cdot t)$, where ω_{d2} is the angular velocity in the S-Plane maneuver. The UCAV keeps $n_{yc}= 1$ and $\theta_u= 0$ during the maneuver.

The barrel roll maneuver is a maneuver that UCAV moves in an S-shaped in both horizontal and vertical planes, of which trajectory characteristics are moving in a circular motion in the vertical plane and at a constant velocity in the forward direction. The control method is given as $n_{yc} = n_{yd} \cdot \cos(\omega_{d3} \cdot t) + cos\theta_u$ in the pitch channel and $n_{zc} = n_{zd} \cdot \sin(\omega_{d3} \cdot t)$ in the yaw channel, respectively, where $n_{yd} = n_{zd}$ and ω_{d3} is the angular velocity in the barrel roll maneuver.

d: TERMINAL TYPE

Terminal type maneuvers are generally used in the final evasive phase when the UCAV is close to the incoming missile, and the most common maneuver is to make a sharp turn toward the missile with a high overload (i.e., last-ditch maneuver). The line-of-sight rate and required overload of the missile can be increased rapidly in this way, thereby improving the probability of successful evasion. The trajectory of the last-ditch maneuver is demonstrated in Fig. 7.

The control method of the last-ditch maneuver in the yaw channel is designed as

$$n_{zc}= sgn(\dot{x}_u \cdot z_r - \dot{z}_u \cdot x_r) \cdot n_{zd} \tag{18}$$

Equation (18) is to turn the UCAV towards the side of the incoming missile. Meanwhile, let $n_{yc}= 1$ during the turn.

In addition, if the velocity of the incoming missile is low in the final evasive phase, the UCAV can evade the missile by maintaining the maneuver of the previous stage to avoid a large EC caused by the last-ditch maneuver. This is also designed as the second maneuver of the terminal type.

C. QUALITATIVE PLANNING AND DECISION SPACE

The evasive strategy is studied qualitatively through modification and combination of timing, type, and parameters of evasive maneuvers in this section. The quantitative optimization of decision space based on the qualitative evasive tactics can guarantee the accuracy, continuity, and interpretability of the evasive trajectory. Meanwhile, it also helps pilots perform the evasive tactical maneuvers preferably in the actual air combat. Compared to the maneuver decision model with fixed period [19], the proposed approach has a more rational decision and execution period. Furthermore, for optimization algorithms, it also avoids the excessive consumption of computing resources caused by the small granularity of maneuver sequences.

According to tactical experiences and analysis result of evasive maneuver models in Section II-B.4, different types of maneuvers are suitable for different timing, there is a certain execution order and priority among them.

In the initial evasive phase, the UCAV should perform turning type maneuvers in the right timing and make the missile behind the tail. The missile is usually far from the UCAV at the beginning of tail-chase geometry. At this point, the purpose of evasive maneuver should be to increase the drag force and the EC of the missile through altitude type maneuvers. Then prolonging the flight time of the missile by period type maneuvers in lower altitudes with greater air density. Meanwhile, period type maneuvers can further accelerate the missile EC and reduce the missile's tracking accuracy in this phase. Compared to a long distance, the line-of-sight rate of the missile caused by evasive maneuvers are relatively larger when the missile is close to the UCAV. Therefore, at this point, terminal type maneuvers should be adopted to rapidly increase the missile's required overload, making it difficult to track the UCAV, thus increasing the terminal MD.

On the one hand, there is no need to traverse the above four types of maneuvers because of the different initial situations. It is selected by a certain priority. In this paper, the tactical maneuver priority is set according to the tactical requirements and maneuver characteristics. The highest

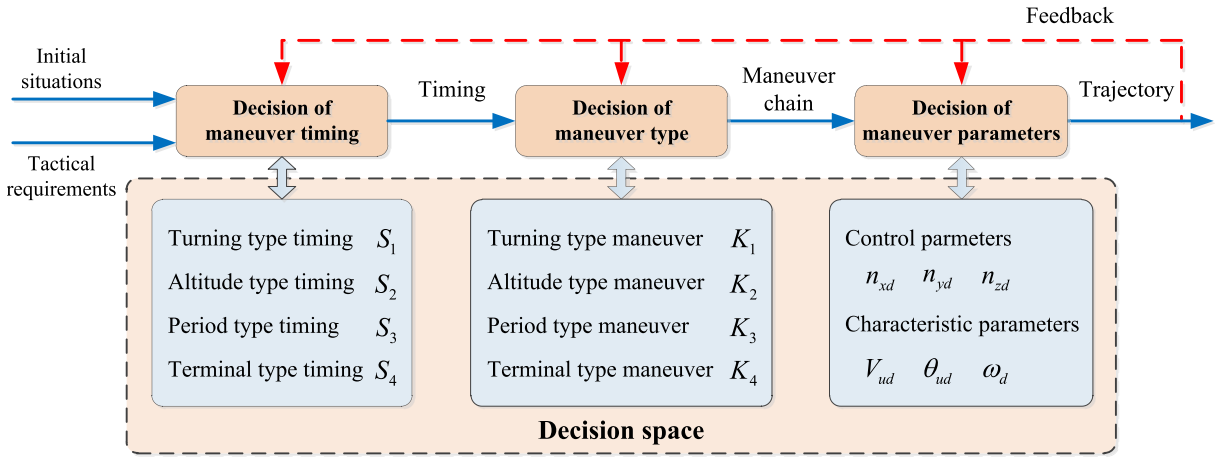

FIGURE 8. The three-level decision space structure.

priority is the terminal type, then followed by the turning type, the altitude type, and the period type in turn. On the other hand, the intensity of evasive maneuver depends on the threat level of the missile (determined by the relative distance and missile's residual energy), and the EC of UCAV is also directly proportional to the intensity. When the threat level of the missile is low, the UCAV can choose a relatively moderate maneuver from each type of maneuver in different evasive phases, such as the out and the altitude hold maneuver. Therefore, the decision of timing, type, and parameters of maneuver needs to balance the relationship between MD, EC, and GST. Based on the above qualitative planning of evasive tactics, the three-level decision space structure is designed as Fig. 8.

As shown in Fig. 8, the complex evasive decision problem is decomposed hierarchically. The decision space structure generates the evasive timing, maneuver chain, and trajectory of the UCAV in turn. Moreover, all variables in decision space can be optimized in parallel according to the evasive objectives and effects.

At the decision level of maneuver timing, when the distance between the UCAV and the missile is $S_1 \cdot r_0$, the UCAV starts to perform turning type maneuvers. That is the moment t_1 in Fig. 1, i.e., the UCAV finishes supporting BM and starts the phase P_e. The value of S_1 represents the length of the UCAV's guidance support phase, where $S_1 \in [0, 1]$ and r_0 is the initial distance when the enemy missile is launched. Similarly, the desired altitude is $S_2 \cdot H_0$ when performing altitude type maneuvers, where H_0 is the initial altitude of the UCAV. The period and terminal type maneuvers of UCAV are triggered respectively when the distance between the UCAV and the missile are $S_3 \cdot r_0$ and $S_4 \cdot r_0$. The value range of S_2, S_3, and S_4 are the same with that of S_1.

At the decision level of maneuver type, K_1, K_2, K_3, and K_4 refer to the sequence number of the maneuver selected for performing in each maneuver type. For example, $K_1 = 1$ denotes performing the out maneuver in turning type, $K_2 = 2$ denotes performing the L-Dive maneuver in altitude type, and so on.

The decision level of maneuver parameters includes control parameters and characteristic parameters. It should be noted that different maneuver requires different parameters, and some parameters can be the default, such as default states of n_{zd} and ω_d in the L-dive maneuver, default states of n_{xd}, n_{yd}, and θ_{ud} in the S-Plane maneuver, and so on.

Moreover, to generate an executable and sequential evasive maneuver chain, it is necessary to ensure the smooth transitions between maneuvers. Therefore, the constraints of switching maneuvers are given by $n_{yc}= 1$ and $\theta_u = 0$, that is, each maneuver is switched to the next one through a horizontal flight.

D. OBJECTIVE SPACE

1) OBJECTIVE FUNCTION MODEL

In the scenario of Fig. 1, the multi-objective of evasive maneuver strategy include: maximizing the MD as much as possible to increase the survival probability, prolonging the GST as much as possible to increase the probability of hitting the target, and decreasing the EC as much as possible for tactical superiority in subsequent combat.

a: MD

The MD is the closest distance between the UCAV and the missile, namely, the distance when the closing velocity is zero. For the evasive UCAV, the most basic objective is to make the MD greater than the missile's damage radius. The damage radius of the missile is simplified to a sphere with a radius of $d_{\max}$ in this paper. To ensure the consistency with other objective functions, the objective function of the MD is defined as

$$J_1 = \begin{cases} 1/r(t_f), & r(t_f) > d_{\max} \\ P, & r(t_f) \le d_{\max} \end{cases} \tag{19}$$

where P is a large constant that represents the punishment for failed evasion of the UCAV. Besides, the terminal time t_f

satisfies the following condition:

$$\dot{r}(t_f) = 0 \tag{20}$$

b: EC

In the normal direction, the EC of UCAV is proportional to the control overload, i.e., n_{yc} and n_{zc}. In the tangential direction, V_u directly reflects the EC of UCAV. Therefore, in this paper, the objective function of EC is modeled as the following form:

$$J_2 = \int_{t_0}^{t_f} \sqrt{(V_u/V_{u\min})^2 + {n_{yc}}^2 + {n_{zc}}^2}dt \tag{21}$$

where t_0 is the initial time.

c: GST

The GST is the flight time of the UCAV from the launch of the enemy missile to the distance between them equals $S_1 \cdot r_0$. In this phase (i.e., the phase P_g in Fig. 1), the UCAV provides guidance information for the missile launched by itself. Therefore, the objective function of GST can be directly defined as

$$J_3 = \begin{cases} 1/t_s, & t_s > 0 \\ 2/T, & t_s = 0 \end{cases} \tag{22}$$

where T is the time step of the simulation. Besides, the interrupt guidance time t_s satisfies the following condition:

$$r(t_s) = S_1 \cdot r_0 \tag{23}$$

The distance between UCAV and the incoming missile is calculated according to (4). It can be seen that S_1 is not only the decision variable but also the influence factor of the objective space.

Combined with the above mentioned multi-objective evasive tactical requirements and the objective functions, the optimization model of evasive maneuver strategy for UCAV in BVR air combat is defined as

$$\begin{cases} \min J(X) = (J_1(X), J_2(X), J_3(X)) \\ X = (S_i, K_i, n_{xd\_ij}, n_{yd\_ij}, n_{zd\_ij}, V_{ud\_ij}, \theta_{ud\_ij}, \omega_{d\_ij}) \\ i = 1, 2, \ldots 4; \quad j = 1, 2, 3 \end{cases} \tag{24}$$

where X is the decision vector. To reduce the value range in decision space and improve optimization efficiency, each decision variable can be set a reasonable value range based on the empirical value. The boundary of the timing and type variable selected for the ith maneuver timing are denoted by $S_i \in [S_{i\min}, S_{i\max}]$ and $K_i \in \{1, 2, 3\}$, respectively. Besides, $K_4 \in \{1, 2\}$. The composition and value range of maneuver parameter variables are determined by maneuver type variable K_i, so the dimension of X is changing dynamically. n_{xd_ij} is the overload of the UCAV in the tangential direction, which belongs to the jth maneuver in the ith maneuver timing. The value range of n_{xd_ij} can be preset as $n_{xd\_ij} \in [n_{xd\_ij\min}, n_{xd\_ij\max}]$ based on experience, other maneuver parameters variables are similarly, such as $n_{yd\_ij} \in [n_{yd\_ij\min}, n_{yd\_ij\max}]$, $V_{ud\_ij} \in [V_{ud\_ij\min}, V_{ud\_ij\max}]$, and so on.

2) END CONDITIONS OF EVASION

According to the established missile and UCAV model, if given the initial situation information of the missile and the UCAV, whether the UCAV can successfully evade the missile can be determined through simulation. Evasive results include the following possible scenarios:

a: FAILED EVASION

In the simulation, if the situation satisfies $r \le d_{\max}$ and other conditions (i.e., the missile velocity and working time of the missile energy), the missile is believed to have hit the aircraft (i.e., a failed evasion). Besides, if the flight trajectory given by the evasive strategy causes UCAV to exceed the height constraint in (11), the evasion is also failed.

b: SUCCESSFUL EVASION

There are also several possible scenarios for UCAV to evade the missile successfully. a) The simulation time t exceeds the maximum working time of the missile energy $t_{\max}$. b) The missile velocity V_m is less than the minimum controlled velocity $V_{m\min}$, which will lead to the self-destruction of the missile as out of control. c) In the terminal phase, if $r > d_{\max}$ when $\dot{r} = 0$. All these scenarios will lead to successful evasion.

III. SOLUTION ALGORITHM DESIGN

It is a complex multi-objective optimization problem with a multi-modal combination to generate the approximate Pareto-optimal evasive maneuver strategy set. Studies have shown that the MOEA/D is effective in dealing with most multi-objective optimization problems [37]. However, the problem in this paper shows the characteristics of a multi-modal combination caused by different physical meanings of decision variables. It is difficult to achieve individual evolution through the traditional strategy of offspring generating. Therefore, the MOEA/D is redesigned in this section, a new HMOEA is proposed to solve the problem in this paper.

A. NORMALIZED DECOMPOSITION MECHANISM

In the MOEA/D, the number of the subproblems is denoted by N, then let $\lambda = (\lambda^1, \lambda^2, \ldots, \lambda^N)$ be a weight vector($\sum_{i=1}^{N} \lambda^i = 1$, $\lambda^i \ge 0$, $i = 1, \ldots, N$), where $\lambda^i = (\lambda_1^i, \lambda_2^i, \lambda_3^i)$. According to the decomposition mechanism in the MOEA/D, the multi-objective optimization problem is decomposed into a series of subproblems $\min g^i(X)(i = 1, 2, \ldots, N)$ through the above weight vector. The objective function of each subproblem is the aggregate function of all objective components. The commonly used aggregation function construction approaches include the weighted sum approach, the boundary intersection approach, and the tchebycheff approach. The weight coefficient and the penalty coefficient of the first two approaches need to be preset through experience or experiment. On this basis, the aggregation function is constructed by the tchebycheff approach in

this paper, then the ith subproblem could be defined as

$$\min g^{te}(X|\lambda^i, z^*) = \max_{1\le j\le 3}\{\lambda_j^i|J_j(X) - z_j^*|\} \tag{25}$$

where $z^* = (z_1^*, z_2^*, z_3^*)$ is the reference point, i.e., $z_j^* = \min J_j(X)(j = 1, 2, 3)$.

In order to reduce the error caused by the dimension difference and value range difference of objective functions in this paper. The value of objective function needs to be performed normalization and mapped to [0, 1], which is calculated by the following equation:

$$\bar{J}_j(X) = \begin{cases} (J_j(X) - z_j^*)/(z_j^{\max} - z_j^*), & if\ z_j^{\max} \neq z_j^* \\ 1, & otherwise \end{cases} \tag{26}$$

where $z_j^{\max} = \max J_j(X)(j = 1, 2, 3)$. To reduce computational complexity, z_j and $\bar{z}_j^{\max}$ are used to approximate z_j^* and $z_j^{\max}$, respectively, where $z_j = \min\{J_j(X)|X \in pop\}$ and $\bar{z}_j^{\max} = \max\{J_j(X)|X \in pop\}$. pop denotes the population of current generation. Therefore, (25) could be designed as

$$\min g^{te}(X|\lambda^i, z^*) = \max_{1\le j\le 3}\left\{\lambda_j^i\left|\frac{J_j(X) - z_j}{\bar{z}_j^{\max} - z_j}\right|\right\} \tag{27}$$

The population in each generation consists of the current optimal solution of each subproblem. The evolutionary operation of each subproblem is limited to its neighborhood, which distances are calculated by the Euclidean distances between any two weight vectors. Thereupon, the new individual will updates its parents and neighborhood simultaneously, so that the better new individuals can be retained to the next generation as much as possible.

B. HIERARCHICAL EVOLUTIONARY MECHANISM

The traditional strategy of offspring generating usually encodes all decision variables into a vector (i.e., chromosome). However, the physical meanings of decision variables are different in this paper, which also have characteristics of coupling and association among them. Meanwhile, the dimension of decision variables is changing dynamically. The traditional strategy is easy to generate a large number of invalid solutions, thereby reducing algorithm efficiency. Therefore, a new hierarchical evolutionary mechanism is designed to generate the new individual in this paper. The basic idea of the mechanism is to classify decision variables according to their physical meanings, code them independently, then put them in different layers (i.e., different populations). Besides, different genetic operators and genetic parameters could be used in different layers. The principle structure is shown in Fig. 9.

According to the decision space structure in Fig. 8, the decision variables are classified into three subpopulations: timing, type and parameters of maneuver, denoted by pop_1, pop_2, and pop_3, respectively. Each subpopulation adopts different coding methods, crossover parameters (i.e., μ_{ci}) and mutation parameters (i.e., p_i, μ_{pi}, $i = 1, 2, 3$) for genetic manipulation. Any subpopulation pop_j includes N subindividuals Ind_{i_j} ($i = 1, 2, \ldots, N$ and $j = 1, 2, 3$). Any complete individual i consists of three independent subindividuals Ind_{i_j}, where Ind_{i_1}, Ind_{i_2}, and Ind_{i_3} denote the subindividual for the decision of timing, type, and parameters of maneuver, respectively. Besides, there is a coupling relationship between the subindividuals in pop_2 and pop_3. The subindividual k_{i_j} in pop_3 denotes parameters code of the maneuver, which corresponding to the jth maneuver in the ith maneuver timing of the subindividual in pop_2. It should be noted that different maneuvers require different parameters, so some parameters can be the default (see Fig. 9).

1) CODING METHOD

The mode of real coding used in this paper can enhance the search capability of evolutionary algorithms. In real coding, the following linear transformation is used for the continuous decision variables in pop_1 and pop_3:

$$x_i = x_i^l + u(0, 1)(x_i^u - x_i^l) \tag{28}$$

The following linear transformation is used for the discrete integer decision variables in pop_2:

$$x_i = x_i^l + int((u(0, 1)(x_i^u - x_i^l))/l_i + 0.5)l_i \tag{29}$$

In (28) and (29), x_i denotes the code of each decision variable, x_i^u and x_i^l denote the upper and lower bounds of each decision variable, respectively. $u(0, 1)$ is the random number evenly distributed within [0, 1], $int(\cdot)$ is the rounding function, l_i is the step size of the decision variable ($l_i = 1$ in this paper).

2) GENETIC MANIPULATION

According to the principle of the hierarchical evolutionary mechanism in Fig. 9, the traditional process of genetic manipulation is improved based on the simulated binary crossover (SBX) and the polynomial mutation (PM) [37].

Firstly, assume that two parents selected randomly in the neighborhood of a subproblem are a and b, where $a, b \in [1, 2, \ldots, N]$. Thereupon, the corresponding parents are Ind_{a_1} and Ind_{b_1} in pop_1, Ind_{a_2} and Ind_{b_2} in pop_2. The parents use SBX operator and corresponding distribution factors(i.e., μ_{c1} and μ_{c2}) to generate new subindividuals in parallel in their respective subpopulations, and the new subindividuals are denoted as Ind'_{c_1} and Ind'_{c_2}.

Because of the coupling relationship stated above, it is necessary to perform the directional crossover and the random inheritance for parents Ind_{a_3} and Ind_{b_3} in pop_3 according to Ind'_{c_2}. That is, the parameters codes of the maneuver represented by Ind'_{c_2} is selected directionally to perform crossover. The other unselected parameter codes (that is represented as the ellipsis in the pop_3 in Fig. 9) randomly inherit from any of two parents by the following equation:

$$x_{ci} = \begin{cases} x_{ai}, & if\ (0, 1) \le 0.5 \\ x_{bi}, & otherwise \end{cases} \tag{30}$$

where x_{ci} denotes unselected parameter codes in Ind'_{c_3}, x_{ai} and x_{bi} denote corresponding unselected parameter codes

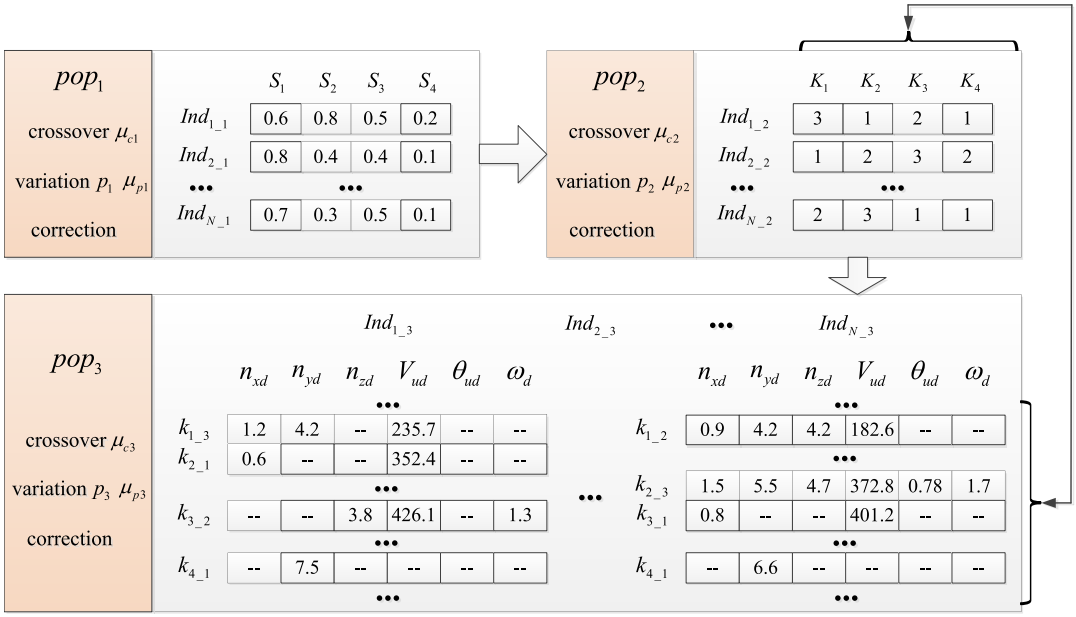

FIGURE 9. The principle structure of the hierarchical evolutionary mechanism.

of parents. For example, in Fig. 9, if the sequence numbers of the parents selected for crossover are 1 and N, and the value K_1 of the new subindividual Ind'_{c_2} changes to 1 by crossing 3 and 2. Then the k_{1_1} of Ind'_{c_3} is selected directionally parameter codes, which value is created by crossing the k_{1_1} of Ind_{1_3} and Ind_{N_3}. Both k_{1_2} and k_{1_3} of Ind'_{c_3} are unselected parameter codes, which values are created by random inheritance according to (30).

Then, the new subindividuals resulting from the above crossover operation Ind'_{c_1}, Ind'_{c_2}, and Ind'_{c_3} use PM operator, corresponding mutation probability (i.e., p_1, p_2, and p_3) and distribution factors (i.e., μ_{p1}, μ_{p2}, and μ_{p3}) to perform mutation operation. Moreover, if the code of Ind'_{c_2} is changed by mutation, selected directionally parameter codes of Ind'_{c_3} will switch accordingly.

When the code of decision variables in a new individual exceed their corresponding boundaries in the process of genetic manipulation. The following equation is used to modify the situation:

$$x_i = \begin{cases} x_i^l + u(0,1)(x_i^l - x_i), & x_i < x_i^l \\ x_i^u - u(0,1)(x_i^u - x_i), & x_i > x_i^u \end{cases} \tag{31}$$

Variables in (31) have the same meanings as that in (28). New subindividuals (i.e., Ind_{c_1}, Ind_{c_2}, and Ind_{c_3}) created by such genetic manipulation as crossover, mutation, and modification make up a complete offspring individual together.

C. ALGORITHM FLOWCHART

The aforementioned normalized decomposition and hierarchical evolution mechanisms combined with the traditional MOEA/D update mechanisms, such as the optimal solution update, the neighborhood solution update, and the external population update [36] constitute the HMOEA framework for solving the evasive maneuver strategy of UCAV in this paper. The algorithm flowchart is shown in Fig. 10.

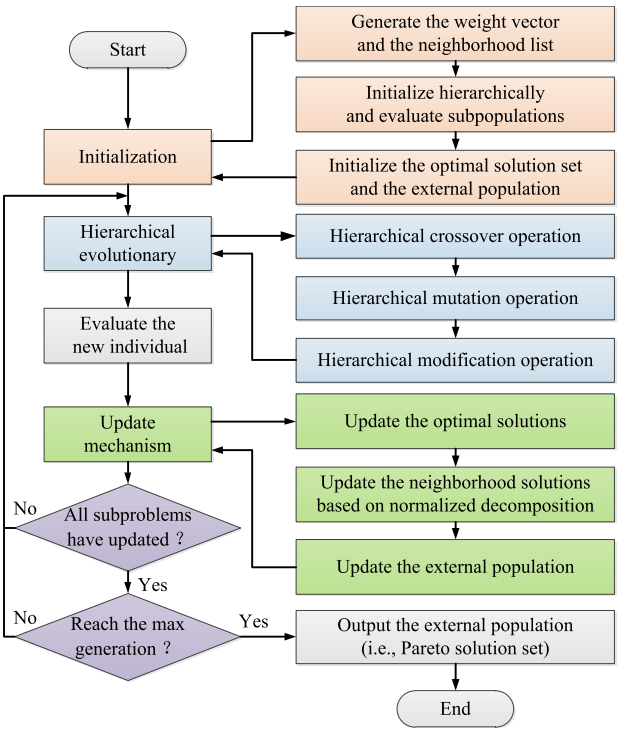

FIGURE 10. The flowchart of the HMOEA.

IV. SIMULATION AND ANALYSIS

To validate the accuracy of models and the effectiveness of the approach in this paper, three simulation experiments are

TABLE 1. Initial states of the UCAV and the missile.

	$x\ (km)$	$z\ (km)$	$y\ (km)$	$V\ (m/s)$	$\theta\ (rad)$	$\phi\ (rad)$
UCAV	0	20	9	250	0	-pi
Missile	50	20	9	300	0	0

performed in this section, and the results are analyzed based on the process of air combat.

Firstly, all initial parameters used in simulations are given in the following Section IV-A. In Section IV-B, the satisfactory initial scenario is designed, then the rationality of the scenario and the accuracy of models are tested by simulation. Then, under the above initial scenario, an ideal strategy set of evasive maneuvers is obtained by the proposed approach in Section IV-C. Finally, in Section IV-D, the feasibility and effectiveness of the proposed approach are further validated through several simulations under different initial scenarios.

A. SIMULATION PARAMETERS

The model parameters of the UCAV and the missile, algorithm parameters, and operating environment parameters are given as follows.

Parameters of the UCAV model are set as $n_{x\max} = 2$, $n_{n\max} = 9$, $y_{u\min} = 0.5km$, $y_{u\max} = 20km$, $V_{u\min} = 200m/s$, $V_{u\max} = 400m/s$, and $T = 0.02s$.

Parameters of the missile model are set as $m_m(0) = 130kg$, $P_m(0) = 13kN$, $t_p = 9s$, $m_m(t_p) = 102kg$, $N_m = 4$, $t_{\max} = 120s$, $n_{\max} = 40$, $\tau_m = 0.2s$, and $V_{m\min} = 400m/s$. To fully guarantee the security of the UCAV, the damage radius of the missile is set to a relatively large value, let $d_{\max} = 50m$.

Parameters of the algorithm are set as following: the max generation, the number of the subproblem, the neighborhood list size, and the external population size are 2000, 500, 40, and 200, respectively. Different genetic parameters are designed according to the actual characteristics of different populations, let $\mu_{c1} = \mu_{c3} = 1$, $\mu_{c2} = 2$, $p_1 = p_3 = 0.2$, $p_2 = 0.1$, $\mu_{p1} = \mu_{p3} = 6$, and $\mu_{p2} = 4$.

All simulation experiments were carried out in MATLAB R2012a environment on a PC with i7-2.5GHz CPU and 4GB memory.

B. SIMULATION EXPERIMENT 1

As previously mentioned, unlike the situation of "endgame evasion", in this research, the UCAV is located outside the missile's GKZ. Meanwhile, not exceed the missile's dynamic-escape zone (DEZ) [33]. In this case, the UCAV cannot successfully evade the missile through a conventional single maneuver. Therefore, according to the missile performance and research needs, initial states of the UCAV and the missile are set as shown in Table 1. The meanings of six variables in Table 1 are similar to (5) and (10), just delete the subscript.

States in Table 1 form a typical initial scenario of BVR air combat, and the scenario is set for a head-on starting geometry, in which both the aspect angle and the flight path angle of the UCAV and missile are set to zero. The geometry is also set with a relative distance of $50km$.

In this simulation experiment, a typical evasive strategy used for the UCAV is set as follows: As the enemy missile is launched, the UCAV immediately performs the out maneuver with a constant initial velocity, and let $n_{zd} = 4$, $\phi_{u0} = 0°$, and $\phi_{ud} = 180°$ in (13). Then it accelerates to $V_{u\max}$ by using $n_{xd} = 2$, followed by the evasion of the CV. It is well known that the above evasive strategy is the most commonly used in actual BVR air combat.

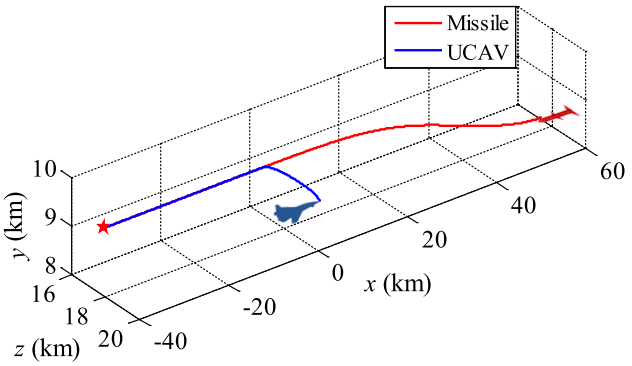

FIGURE 11. Three-dimensional trajectories of the UCAV and the missile with typical evasive strategy.

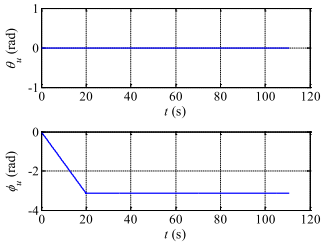

FIGURE 12. Time history of the UCAV's track angle.

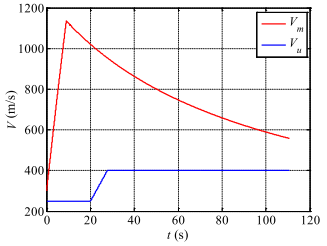

FIGURE 13. Time history of velocity of vehicles.

Based on the above simulation parameters and the initial scenario, the simulation results are shown in Fig. 11-Fig. 15.

Simulation results show that the UCAV is hit by the missile at $114.06s$. The red star in Fig. 11 denotes the missile's explosion point (the UCAV is hit. $t > t_{\max}$ or $V_m < V_{m\min}$ will also triggers the explosion of the missile, similarly hereinafter).

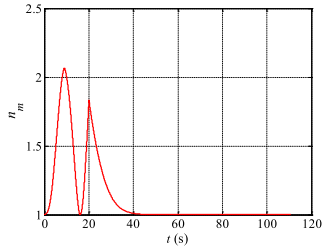

FIGURE 14. Time history of the missile's normal overload.

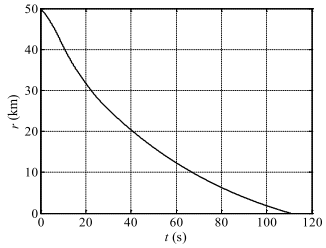

FIGURE 15. Time history of the relative distance.

As showed in Fig. 11 and Fig. 12, θ_u is always zero in the whole process, ϕ_u is changing from 0 to $-180deg$ in less than $20s$ during the evasion. Meanwhile, the interception geometry is changing from a head-on to a tail-chase geometry. It's noted from Fig. 13, the time history of the UCAV's velocity is consistent with the above strategy. The missile is in the passive deceleration state after the active acceleration of t_p. End condition of $t_{\max}$ or $V_{m\min}$ is not triggered. According to Fig. 14, the normal overload of the missile does not change much, especially it equals 1 in the tail-chase phase. Moreover, the relative distance r gradually decreases from $r_0 = 50km$ to $r \in [0, d_{\max}]$ (see Fig. 15).

As regards the above three evasive tactical objectives, the UCAV is hit in this simulation experiment, so there is no practical meaning to consider EC. Besides, since the UCAV performs the out maneuver immediately, its GST is zero, i.e., the probability of hitting the target is also relatively low. In general, the whole combat efficiency of UCAV is pretty low.

On the one hand, this simulation experiment provides the research foundation for the subsequent algorithm verification through the test of models and the initial scenario. On the other hand, it illustrates that the typical evasive strategy cannot accomplish the evasive task, let alone multiple tactical objectives.

C. SIMULATION EXPERIMENT 2

As a comparative study, the initial scenario in this simulation experiment is the same with that of Section IV-B. The main difference is that the evasive strategy is given by the optimization model and algorithm proposed in this paper.

An approximate Pareto front is obtained through digital simulation (see Fig. 16), it shows a set of nondominated

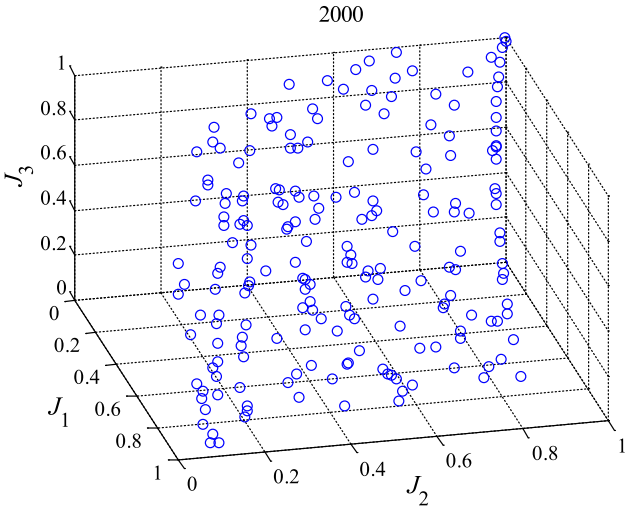

FIGURE 16. Plot of the approximate Pareto front.

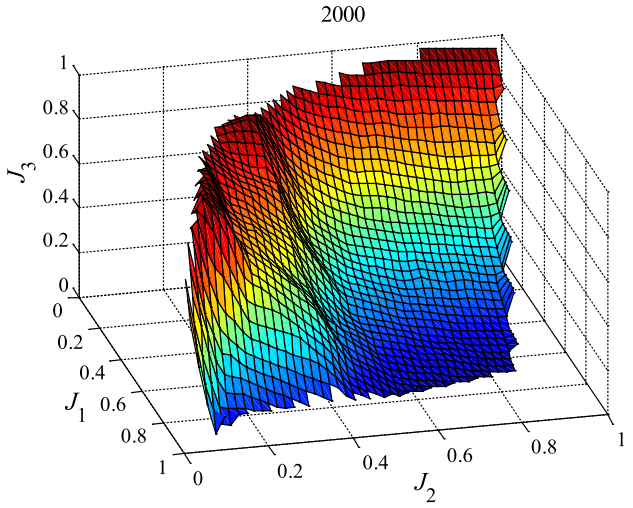

FIGURE 17. Fitted surface of the approximate Pareto front.

solutions which reflect the different evasive tactical requirements of UCAV while ensuring successful evasion. Each nondominanted solution in Fig. 16 represents a strategy with a structure as shown in Fig. 8. It also represents a feasible evasive flight path. The values of the three objective functions in Fig. 16 are normalized, and the boundary values of the MD, EC, and GST are $[0.0531,\ 13.4111]km$, $[272.651,\ 603.245]$, and $[0,\ 15.20]s$, respectively. To observe the changing trend of the approximate Pareto front more intuitively, through the Curve Fitting Tool in Matlab2012a, the data in Fig. 16 is generated into the fitted surface as shown in Fig. 17.

As seen in Fig. 17, if given one of the three values of the objective functions, in the two remaining values, better in one will lead to worse in the other. This validate the self-conflicting characteristic of the proposed three optimization objectives in the problem of evasive strategy in BVR air combat.

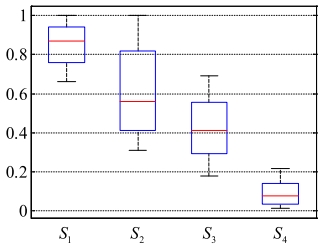

FIGURE 18. Box plot of timing variables of evasive maneuvers in the nondominated solution set.

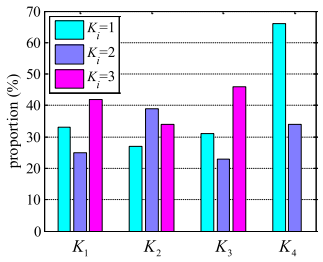

FIGURE 19. Histogram of type variables of evasive maneuvers in the nondominated solution set.

Furthermore, the distribution characteristics of the decision variables in the obtained nondominanted strategy set can be seen in Fig. 18 and Fig. 19.

According to Fig. 18, the distribution range of S_1, S_3, and S_4 are in accordance with the order from large to small. This indicates the rationality and effectiveness of performing the turning, period, and terminal type maneuvers in the early, middle, and end phases of evasion, respectively. The distribution of S_2 also reflects the positive effect of altitude reduction on the evasion. The split-S maneuver, L-Dive maneuver, barrel roll maneuver, and last-ditch maneuver account for the highest proportion of performing in their respective maneuver type, and other maneuvers also account for a certain proportion. It shows that each maneuver has its advantageous region, the effectiveness of evasive maneuver models are also verified. Different evasive trajectories and corresponding objective function values are determined by modification and combination of timing, type, and parameters of evasive maneuvers, which result in different tendency of evasive tactics.

The following are the simulation and analysis of the optimal solutions of the three objectives.

1) THE OPTIMAL MD

According to the calculation results in Fig. 16, it can be obtained that the optimal MD in the nondominated solution set is 13.4111km, of which decision set are shown in Table 2.

Based on the initial scenario in Table 1 and the decision set in Table 2, the simulation results are shown in Fig. 20-Fig. 22.

Simulation results show that the missile triggers a self-destruction caused by $V_m < V_{m\min}$ at 104.24s and the MD is 13.4111km.

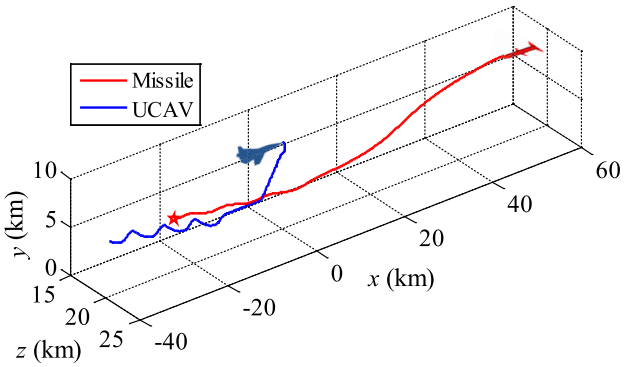

FIGURE 20. Three-dimensional trajectories of the UCAV and the missile when MD is optimal.

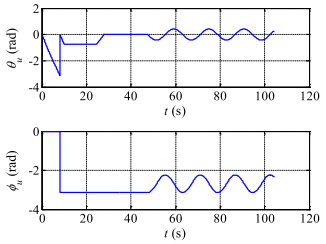

FIGURE 21. Time history of the UCAV's track angle.

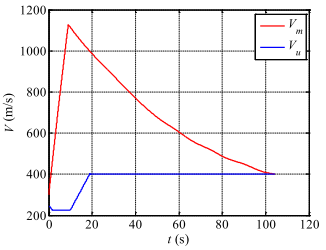

FIGURE 22. Time history of velocity of vehicles.

It can be seen from Fig. 20 and Fig. 21 that the UCAV performs a split-S maneuver with high overload immediately after the missile is launched, and the tail-chase geometry quickly formed within 8.2s. The turning efficiency is much higher than that in simulation experiment 1. The jump of the UCAV's track angle between 0rad and $-3.14rad$ at 8.2s is caused by the defined range of track angle, it's actually continuous (similarly hereinafter). Then it performs the L-Dive maneuver with $\theta_{ud} = -0.72rad$, followed by a horizontal flight with the velocity of $V_{u\max}$ at the altitude of $r_0 \cdot S_2 = 3.87km$. Until the relative distance r is $r_0 \cdot S_3 = 22.5km$, the UCAV starts the barrel roll maneuver. The periodic change of the UCAV's track angle can be seen in Fig. 21. As the MD is greater than the trigger distance of the terminal type maneuvers in the decision set, the terminal maneuver is not performed. It's noted from Fig. 22 that the UCAV turns with deceleration and then accelerates to $V_{u\max}$. Besides, the deceleration effect of the missile is more obvious than

TABLE 2. Decision set for the optimal MD.

S_1	S_2	S_3	S_4	K_1	K_2	K_3	K_4	n_{xd_13}	n_{yd_13}	V_{ud_13}	n_{xd_22}	n_{yd_22}	V_{ud_22}	θ_{ud_22}	n_{zd_33}	V_{ud_33}	ω_{d_33}	n_{zd_41}
1	0.43	0.45	0.05	3	2	3	1	-1.6	-9	226	2	-9	400	-0.72	-6.9	400	0.4	-7.5

TABLE 3. Decision set for the optimal EC.

S_1	S_2	S_3	S_4	K_1	K_2	K_3	K_4	n_{xd_11}	n_{zd_11}	V_{ud_11}	n_{xd_22}	n_{yd_22}	V_{ud_22}	θ_{ud_22}	n_{xd_31}	V_{ud_31}
1	0.61	0.34	0.03	1	2	1	2	-1.5	-4.2	200	1.1	-1.6	233	-0.78	1.6	360

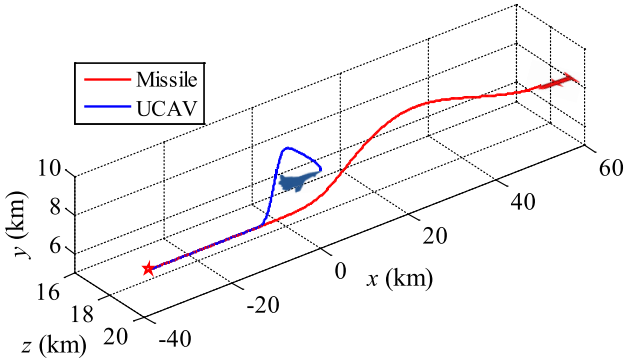

FIGURE 23. Three-dimensional trajectories of the UCAV and the missile when EC is optimal.

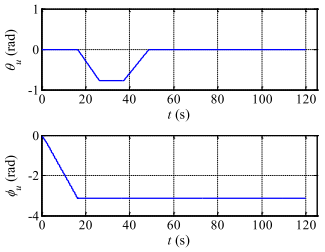

FIGURE 24. Time history of the UCAV's track angle.

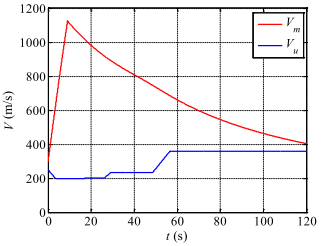

FIGURE 25. Time history of velocity of vehicles.

that in simulation experiment 1, the major reason is the larger drag force of the missile in lower altitude.

As regards the tactical objectives, the objective function value of the EC and the GST is 603.245 and 0, respectively. Therefore, the evasive trajectory of optimal MD can guarantee the maximum survival probability of UCAV, but it also means that the probability of hitting the target is relatively low. Furthermore, the large EC also leads to relatively less tactical superiority in subsequent air combat.

2) THE OPTIMAL EC

According to the calculation results in Fig. 16, it can be obtained that the optimal EC in the nondominated solution set is 272.651, of which decision set are shown in Table 3.

Based on the initial scenario in Table 1 and the decision set in Table 3, the simulation results are shown in Fig. 23-Fig. 25.

Simulation results show that the missile triggers a self-destruction caused by $t > t_{\max}$ and the MD is $0.0531km$.

It can be seen from Fig. 23 and Fig. 24 that the UCAV performs the out maneuver with light overload immediately after the missile is launched, the turning takes nearly $20s$ and then the L-Dive maneuver starts with $\theta_{ud} = -0.78rad$, followed by a horizontal flight at the altitude of $r_0 \cdot S_2 = 5.49km$. Afterwards, UCAV accelerates to $360.2m/s$ by the CA maneuver in the period type maneuver. In the terminal phase, UCAV continues the horizontal flight state of the previous phase. It's noted from Fig. 25, the UCAV never use the maximum velocity during the whole process, and the altitude is relatively higher than that in Fig. 20. So the deceleration effect of the missile is relatively slow, which results in a corresponding increase in the evasive time.

As regards the tactical objectives, compared with the strategy of the optimal MD, this strategy saves more than half of the energy for the UCAV, and fully guarantees the tactical superiority in subsequent air combat. However, the zero GST and the small MD also lead to relatively low probability both of survival and hitting the target.

3) THE OPTIMAL GST

According to the calculation results in Fig. 16, it can be obtained that the optimal GST in the nondominated solution set is $15.20s$, of which decision set are shown in Table 4.

Based on the initial scenario in Table 1 and the decision set in Table 4, the simulation results are shown in Fig. 26-Fig. 28.

Simulation results show that the missile triggers a self-destruction caused by $V_m < V_{m\min}$ at $104.80s$ and the MD is $0.0846km$.

TABLE 4. Decision set for the optimal GST.

S_1	S_2	S_3	S_4	K_1	K_2	K_3	K_4	n_{xd_13}	n_{yd_13}	V_{ud_13}	n_{xd_23}	n_{yd_23}	n_{zd_23}	V_{ud_23}	θ_{ud_23}	ω_{d_23}	n_{zd_33}	V_{ud_33}	ω_{d_33}	n_{zd_41}
0.66	0.36	0.65	0.068	3	3	3	1	-1.5	-9	237	2	-9	-5.65	400	-0.86	0.8	-5.0	400	0.59	-8.9

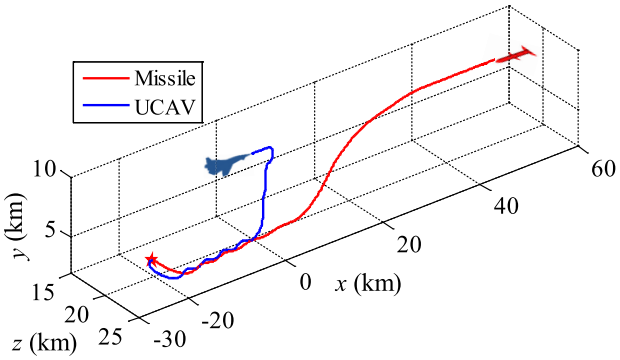

FIGURE 26. Three-dimensional trajectories of the UCAV and the missile when GST is optimal.

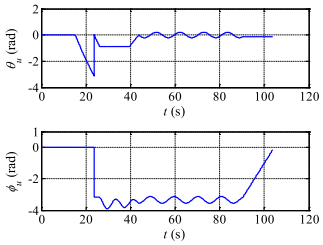

FIGURE 27. Time history of the UCAV's track angle.

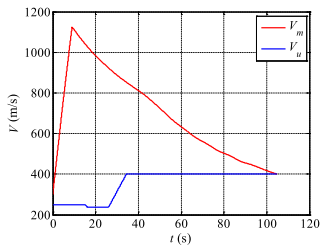

FIGURE 28. Time history of velocity of vehicles.

It can be seen from Fig. 26 and Fig. 27 that the UCAV keeps the initial flight state to guide its own missile after the enemy missile is launched, until the relative distance r is $r_0 \cdot S_1 = 33km$, and the GST in this phase is $15.20s$. Then the UCAV performs a split-S maneuver with high overload to form the tail-chase geometry. Since the UCAV is relatively close to the missile after the split-S maneuver, it uses the S-Dive maneuver to make the missile normal overload periodically change along with the altitude reduction, thereby consuming the missile's energy. Besides, the desired altitude is $r_0 \cdot S_2 = 3.24km$. The period type maneuvers are triggered during the process of altitude reduction, so the UCAV performs the barrel roll maneuver immediately after the S-Dive maneuver. Finally, the UCAV starts the last-ditch maneuver when the relative distance r is $r_0 \cdot S_4 = 3.4km$.

As regards the tactical objectives, this strategy provides longer GST for UCAV, which ensures the probability of hitting the target to a large extent. However, the large EC (i.e., 602.18) and the small MD also bring adverse effects to the survival probability and the tactical superiority in subsequent air combat, respectively.

The simulation result of the missile's normal overload and the relative distance under the three conditions mentioned above is shown in Fig. 29 and Fig. 30, respectively.

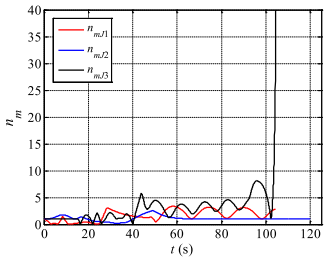

FIGURE 29. Time history of the missile's normal overload.

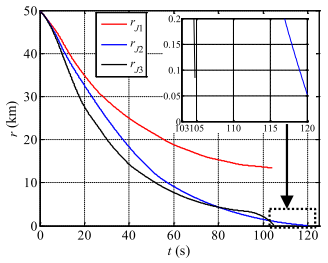

FIGURE 30. Time history of the relative distance.

In Fig. 29, n_{mJ1}, n_{mJ2}, and n_{mJ3} represent the curve of the missile's normal overload under the condition of optimal MD, optimal EC and optimal GST of UCAV, respectively. Similarly, r_{J1}, r_{J2}, and r_{J3} in Fig. 30 represent the corresponding curve of the relative distance. It can be seen from Fig. 29 that both n_{mJ1} and n_{mJ3} are higher than n_{mJ2} in the middle and later periods. This means that the missile's energy decreases rapidly, and the periodic change of the missile's normal overload caused by the periodic maneuver of UCAV also accelerates this decrease. It's worth noting that the last-ditch maneuver leads to the missile's normal overload surge to the limit $n_{\max}$ in n_{mJ3}. According to Fig. 30, r_{J3} declines rapidly in the early evasive phase due to the phase of

TABLE 5. The simulation results based on different initial scenarios.

Missile \ UCAV	0°			15°			30°		
	z_1	z_2	z_3	z_1	z_2	z_3	z_1	z_2	z_3
$-30°$	0.0696	261.02	0.0607	0.0709	262.72	0.0618	0.0700	258.13	0.0611
$-15°$	0.0725	266.86	0.0634	0.0718	264.19	0.0624	0.0688	253.92	0.0604
$-0°$	0.0746	272.65	0.0658	0.0710	261.18	0.0613	0.0670	248.57	0.0579
$15°$	0.0726	266.94	0.0635	0.0692	257.05	0.0600	0.0646	242.66	0.0558
$30°$	0.0698	261.12	0.0608	0.0660	252.41	0.0577	0.0617	238.15	0.0541

guidance support. Besides, the MD of r_{J1} is the largest, the GST of r_{J2} is the longest.

The results and analysis of this simulation experiment validate the both feasibility and effectiveness of the proposed approach for solving the evasive maneuver problem in BVR air combat. The obtained nondominanted solutions all are feasible evasive strategies, and different evasive strategies have different tactical superiority and tendencies. The strategy should be determined according to the current air combat scenario and tactical requirements, so as to achieve the desired tactical objectives, as well as ensure air superiority and the whole combat efficiency while evasive successfully.

D. SIMULATION EXPERIMENT 3

In order to further validate the proposed approach, several simulations under different initial scenarios are carried out in this section, which the UCAV is attacked by the missile from the same altitude, same distance and different directions. The simulation results are shown in Table 5.

The heading angle of the missile varies from $-30deg$ to $+30deg$ with the interval of $15deg$. Because the situation is the same in symmetric scenario, only the scenario of turning right is considered for the UCAV. The heading angle of the UCAV varies from $0deg$ to $30deg$ with the interval of $10deg$. These are common initial scenarios of BVR air combat, and the initial scenario in simulation experiment 1 and 2 correspond to the head-on geometry where the heading angle of both the missile and UCAV are $0deg$.

z_1, z_2, and z_3 in Table 5 represent the optimal value of J_1, J_2, and J_3 in the obtained nondominanted solutions. It can be seen from Table 5, the value of each objective function is the largest in the scenario where the heading angle of both the missile and the UCAV are $0deg$, which is the worst-case scenario for evasion. As the heading angle of both sides deviates from the head-on state, the value of each objective function decreases gradually. When the heading angle of both the missile and the UCAV are $30deg$, the value of each objective function reaches the minimum, that is, it is the most favorable case to evade. It's worth noting that the variation of the heading angle of the UCAV has a larger effect on the evasive results than that of the heading angle of the missile.

The results and analysis in this simulation experiment further validate the both feasibility and effectiveness of the proposed approach. Furthermore, it is of guiding significance to the research the decision of attacking maneuver for UCAV in BVR air combat. Moveover, it also helps pilots perform the evasive tactical maneuvers preferably in the actual air combat.

V. CONCLUSION AND FUTURE WORK

Ensuring tactical superiority and survival probability in BVR air combat are critical to UCAV. This paper studies the autonomous evasive maneuver strategy of the UCAV to evade BVR AAM. The proposed novel approach combines qualitative tactical experience and quantitative maneuver decision optimization method effectively. The amalgamative tactical demands of achieving self-conflicting evasive objectives in actual BVR air combat are also taken into account. The objectives include the MD, the EC and the GST. They responds directly to the survival probability, the superiority in subsequent air combat and the probability of hitting the target, respectively. In this approach, effective maneuvers of UCAV used in different evasion phases are modeled in three-dimensional space, and the three-level decision space structure is established according to qualitative evasive tactical planning. On this basis, the HMOEA is designed to solve the aforementioned problem. Using scenario-based simulations, a set of nondominated evasive strategies is derived, which satisifies a variety of evasive tactical requirements of UCAV while ensuring successful evasion. Besides, because the obtained results in this paper are easy to interpret, they also have practical guiding significance for pilots to perform the evasive tactical maneuvers preferably in the actual air combat. In general, the proposed models and algorithm are feasible and effective for solving the problem of evasive maneuver strategy for UCAV in BVR air combat.

It is necessary to note that, the simulation experiment 2 takes 2.3 hours based on the operating environment parameters given in Section IV-A, so it is difficult to meet the real-time requirements of online application through the computer configuration in Section IV-A. Therefore, the proposed algorithm can be used for off-line calculation in a variety of scenarios, and the results could be loaded into the UCAV computer. It can select the corresponding decision set to perform evasive maneuver online according to the current scenario and tactical requirements. Furthermore, the results could be applied for the UCAV or the manned fighter in the daily BVR air combat evasive tactics training to improve combat efficiency.

Moreover, considering the uncertainty of information and building more accurate models are also the focus and direction of future research.

REFERENCES

[1] T. Yomchinda, "A study of autonomous evasive planar-maneuver against proportional-navigation guidance missiles for unmanned aircraft," in *Proc. Asian Conf. Defence Technol. (ACDT)*, Apr. 2015, pp. 210–214.
[2] Z. Deyun, Y. Zhen, and Z. Kun, "Method of guidance handover in beyond-visual-range coordinated air combat for multi-UCAVs," *J. Ballistics*, vol. 29, no. 2, pp. 1–7, 2017.
[3] K. Horie and B. A. Conway, "Optimal fighter pursuit-evasion maneuvers found via two-sided optimization," *J. Guid., Control, Dyn.*, vol. 29, no. 1, pp. 105–112, Jan. 2006.
[4] R. W. Carr, R. G. Cobb, M. Pachter, and S. Pierce, "Solution of a Pursuit–Evasion game using a near-optimal strategy," *J. Guid., Control, Dyn.*, vol. 41, no. 4, pp. 841–850, Apr. 2018.
[5] F. Imado and T. Kuroda, "Family of local solutions in a missile-aircraft differential game," *J. Guid., Control, Dyn.*, vol. 34, no. 2, pp. 583–591, Mar. 2011.
[6] D. Alkaher and A. Moshaiov, "Game-based safe aircraft navigation in the presence of energy-bleeding coasting missile," *J. Guid., Control, Dyn.*, vol. 39, no. 7, pp. 1539–1550, Jul. 2016.
[7] F. Imado, "Some practical approaches to pursuit-evasion dynamic games," *Cybern. Syst. Anal.*, vol. 38, no. 2, pp. 276–291, 2002.
[8] F. Imado, "Some aspects of a realistic three-dimensional pursuit-evasion game," *J. Guid., Control, Dyn.*, vol. 16, no. 2, pp. 289–293, Mar. 1993.
[9] F. Imado and T. Kuroda, "Engagement tactics for two missiles against an optimally maneuvering aircraft," *J. Guid., Control, Dyn.*, vol. 34, no. 2, pp. 574–582, Mar. 2011.
[10] S. Y. Ong and B. L. Pierson, "Optimal evasive aircraft maneuvers against a sam guided by proportional navigation," in *Proc. AIAA Guid., Navigat., Control Conf. Exhibit*. Reston, VA, USA: AIAA, 1992, p. 4384.
[11] S. Y. Ong and B. L. Pierson, "Optimal planar evasive aircraft maneuvers against proportional navigation missiles," *J. Guid., Control, Dyn.*, vol. 19, no. 6, pp. 1210–1215, Nov. 1996.
[12] J. Karelahti, K. Virtanen, and T. Raivio, "Near-optimal missile avoidance trajectories via receding horizon control," *J. Guid., Control, Dyn.*, vol. 30, no. 5, pp. 1287–1298, Sep. 2007.
[13] J. Karelahti and K. Virtanen, "Adaptive controller for the avoidance of an unknownly guided air combat missile," in *Proc. 46th IEEE Conf. Decis. Control*, Dec. 2007, pp. 1306–1313.
[14] L. Singh, "Autonomous missile avoidance using nonlinear model predictive control," in *Proc. AIAA Guid., Navigat., Control Conf. Exhibit*. Reston, VA, USA: AIAA , Aug. 2004, p. 4910.
[15] L. Fei, Y. Lei, and Z. Zhongliang, "The nonlinear model predictive control avoidance strategy of the fighter maneuver in endgame," *J. Nat. Univ. Defense Technol.*, vol. 36, no. 3, pp. 83–90, 2014.
[16] I. F. Nusyirwan and C. Bil, "Effect of uncertainties on UCAV trajectory optimisation using evolutionary programming," in *Proc. Inf., Decis. Control*, Feb. 2007, pp. 219–223.
[17] F. W. Moore and O. N. Garcia, "A genetic programming methodology for missile countermeasures optimization under uncertainty," in *Proc. Int. Conf. Evol. Program.* Springer, 1998, pp. 365–376.
[18] F. W. Moore and O. N. Garcia, "A new methodology for optimizing evasive maneuvers under uncertainty in the extended two-dimensional pursuer/evader problem," in *Proc. 9th IEEE Int. Conf. Tools with Artif. Intell.*, Nov. 1997, pp. 278–285.
[19] I. Nusyirwan and C. Bil, "Factorial analysis of a real time optimisation for pursuit-evasion problem," in *Proc. 46th AIAA Aerosp. Sci. Meeting Exhibit*, Jan. 2008, p. 199.
[20] H.-L. Choi, H.-C. Bang, and M.-J. Tahk, "Co-evolutionary optimization of three-dimensional target evasive maneuver against a proportionally guided missile," in *Proc. Congr. Evol. Comput.*, vol. 2, 2001, pp. 1406–1413.
[21] W. Xiao-Ping, L. Qin-Ying, and D. Xin-Min, "Aircraft evasive maneuver trajectory optimization based on QPSO," in *Proc. Int. Congr. Ultra Modern Telecommun. Control Syst.*, Oct. 2010, pp. 416–420.
[22] F. Imado and S. Miwa, "Fighter evasive maneuvers against proportional navigation missile," *J. Aircr.*, vol. 23, no. 11, pp. 825–830, Nov. 1986.
[23] F. Imado and S. Miwa, "Three dimensional study of evasive maneuvers of a fighter against a missile," in *Proc. Astrodynamics Conf.*, Aug. 1986, p. 2038.
[24] F. Imado and S. Miwa, "Missile guidance algorithm against high-g barrel roll maneuvers," *J. Guid., Control, Dyn.*, vol. 17, no. 1, pp. 123–128, Jan. 1994.
[25] F. Imado and S. Uehara, "High-g barrel roll maneuvers against proportional navigation from optimal control viewpoint," *J. Guid., Control, Dyn.*, vol. 21, no. 6, pp. 876–881, Nov. 1998.
[26] R. Akdag and T. Altilar, "A comparative study on practical evasive maneuvers against proportional navigation missiles," in *Proc. AIAA Guid., Navigat., Control Conf. Exhibit.*, Aug. 2005, p. 6352.
[27] R. Akdag and D. Altilar, "Modeling evasion tactics of a fighter against missiles in three dimensions," in *Proc. AIAA Guid., Navigat., Control Conf. Exhibit.* Reston, VI, USA: AIAA, Aug. 2006, p. 6604.
[28] Y. Xizhong and A. Jianliang, "Evasive maneuvers against missiles for unmanned combat aerial vehicle in autonomous air combat," *J. Syst. Simul.*, vol. 30, no. 5, p. 1957, 2018.
[29] D. Lee and H. Bang, "Planar evasive aircrafts maneuvers using reinforcement learning," in *Intelligent Autonomous Systems 12*. Springer, 2013, pp. 533–542.
[30] A. Vermeulen and G. Maes, "Missile avoidance maneuvres with simultaneous decoy deployment," in *Proc. AIAA Guid., Navigat., Control Conf.* Reston, VI, USA: AIAA, Aug. 2009, p. 6277.
[31] A. Ratnoo and T. Shima, "Line-of-Sight interceptor guidance for defending an aircraft," *J. Guid., Control, Dyn.*, vol. 34, no. 2, pp. 522–532, Mar. 2011.
[32] T. Shima, "Optimal cooperative pursuit and evasion strategies against a homing missile," *J. Guid., Control, Dyn.*, vol. 34, no. 2, pp. 414–425, Mar. 2011.
[33] D. Alkaher and A. Moshaiov, "Dynamic-escape-zone to avoid energy-bleeding coasting missile," *J. Guid., Control, Dyn.*, vol. 38, no. 10, pp. 1908–1921, Oct. 2015.
[34] J. Karelahti, K. Virtanen, and T. Raivio, "Game optimal support time of a medium range air-to-air missile," *J. Guid., Control, Dyn.*, vol. 29, no. 5, pp. 1061–1069, Sep. 2006.
[35] D. Alkaher and A. Moshaiov, "Nondominated strategies for cautious to courageous aerial navigation," *J. Guid., Control, Dyn.*, vol. 41, no. 7, pp. 1485–1501, Jul. 2018.
[36] Q. Zhang and H. Li, "MOEA/D: A multiobjective evolutionary algorithm based on decomposition," *IEEE Trans. Evol. Comput.*, vol. 11, no. 6, pp. 712–731, Dec. 2007.
[37] H. Li and Q. Zhang, "Multiobjective optimization problems with complicated Pareto sets, MOEA/D and NSGA-II," *IEEE Trans. Evol. Comput.*, vol. 13, no. 2, pp. 284–302, Apr. 2009.

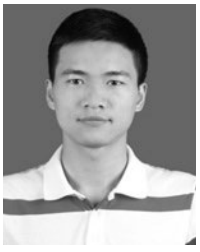

ZHEN YANG received the B.Sc. and M.Sc. degrees in system and control engineering from Northwestern Polytechnical University (NPU), Xi'an, China, in 2014 and 2017, respectively, where he is currently pursuing the Ph.D. degree. He has authored four refereed international journal articles and three peer-reviewed international conference papers to date. His current research interests are intelligent air combat system modeling and simulation, autonomous maneuvering decision-making, and avionics system simulation and testing.

DEYUN ZHOU received the bachelor's, master's, and Ph.D. degrees from Northwestern Polytechnical University (NPU), Xi'an, China, in 1985, 1988, and 1991, respectively. He has been a Professor with NPU, since 1997, where he is currently the Dean of the School of Electronics Information. His current research interests are integrated control theory and application, information fusion, and intelligent information processing.

HAIYIN PIAO received the B.Sc. degree in computer science and automation from the Dalian University of Technology (DLUT). He is currently pursuing the Ph.D. degree with Northwestern Polytechnical University (NPU). His current research interests are multiagent reinforcement learning, game theory, and AI air combat applications.

KAI ZHANG received the B.Sc. and M.Sc. degrees in system and control engineering from Northwestern Polytechnical University (NPU), Xi'an, China, in 2011 and 2014, respectively, where he is currently pursuing the Ph.D. degree with Northwestern Polytechnical University. He has authored three refereed international journal articles and five peer-reviewed international conference papers to date. His current research interests are multiobjective optimization, decision making, and intelligent air combat systems.

WEIREN KONG received the M.Sc. degree in electronics science and technology from Northwestern Polytechnical University (NPU), Xi'an, China, in 2016, where he is currently pursuing the Ph.D. degree. His current research interests are multiagent-based reinforcement learning for multiUAV air combat confrontation decision-making, modeling and simulation of complex systems, and UAV trajectory tracking control.

QIAN PAN received the B.Sc. and M.Sc. degrees in system and control engineering from Northwestern Polytechnical University (NPU), Xi'an, China, in 2011 and 2014, respectively, where he is currently pursuing the Ph.D. degree. From 2016 to 2017, he was a full-time Visiting Postgraduate Student with The University of British Columbia at Okanagan, Okanagan, BC, Canada. He has authored four refereed international journal articles and ten peer-reviewed international conference papers to date. His current research interests are information fusion, intelligent control, decision making, and clustering analysis.